We are IntechOpen,
the world's leading publisher of
Open Access books
Built by scientists, for scientists

4,800
Open access books available

122,000
International authors and editors

135M
Downloads

Our authors are among the

154
Countries delivered to

TOP 1%
most cited scientists

12.2%
Contributors from top 500 universities

CLARIVATE ANALYTICS
BOOK CITATION INDEX
INDEXED

WEB OF SCIENCE™

Selection of our books indexed in the Book Citation Index
in Web of Science™ Core Collection (BKCI)

Interested in publishing with us?
Contact book.department@intechopen.com

Numbers displayed above are based on latest data collected.
For more information visit www.intechopen.com

Preparation of Existing and Novel Superconductors using a Spatial Composition Spread Approach

Kevin C. Hewitt, Robert J. Sanderson and Mehran Saadat
Dalhousie University, Department of Physics and Atmospheric Science, Halifax NS
Canada

1. Introduction

We describe in this chapter a promising system and method to search for novel superconductors by investigating appropriately chosen antiferromagnets and creating carriers by doping using a high throughput spatial composition spread (combinatorial) approach. The method has been applied to the cuprate superconductors and has the potential to enhance our understanding of these materials and push the boundaries of the field by quickly exploring novel ones.

Finding novel superconducting materials, which superconduct at much higher temperatures, now seems to be a realistic goal because of three recent developments: the 2008 discovery of superconductivity in iron arsenide based materials; the observation that a number of superconductors are doped antiferromagnets; and the tremendous progress researchers have made over the past 20 years in understanding the physical properties of existing superconductors. These developments suggest a path to novel superconductors - explore the electrical transport properties of doped antiferromagnets. While a number of applications of existing superconductors have been realized, their widespread use depends on raising the transition temperatures substantially above the current world record T_c of 138 K.

Expanding the number of known systems which exhibit superconductivity also allows researchers to identify its essential elements. These observations help reduce the number of models which purport to explain the mechanism of pair formation, and allow researchers to ignore irrelevant peculiarities of a particular system. In general, the preparation of novel phases of matter increases the likelihood of the discovery of novel material properties. The combinatorial approach to materials discovery (Xiang et al, 1995) allows one to realize these goals at an unprecedented rate.

Discoveries by groups in Japan and China over the past few years have added to the class of systems for which antiferromagnetic order exists in close proximity to superconductivity, and in some cases may even coexist. Iron arsenide-based, cuprate, fulleride and heavy fermion superconductors [detailed references below] populate this class, and the diversity of hosts highlight how useful it is to search for new examples of superconductors in aid of an empirical identification of the important parameters on which to build a correct theory. As the number of examples has grown, the importance of spin fluctuations has emerged. This chapter describes a route to discover novel superconductors in doped antiferromagnets to enhance our understanding of superconductivity. To accomplish these goals we use a

combinatorial approach to materials discovery, which we have recently demonstrated allows us to map the superconducting properties of the La214 cuprate superconductor and search for new superconductors by quickly and efficiently exploring phase space in a chosen system. The single layer K_2CuF_4 and double layer $K_3Cu_2F_7$ perovskites will be shown to be likely candidates to exhibit superconductivity on the border of antiferromagnetic or ferromagnetic phases. Rapid characterization using high throughput resistivity apparatus, such as the one (Hewitt et al, 2005) developed in our lab, allows one to identify superconducting phases at an accelerated pace.

The spatial composition spread approach is described in section 2, its application to cuprate superconductors in section 3 and section 4 proposes likely superconductors on the boundary of antiferromagnetic and ferromagnetic phases.

2. Spatial composition spread approach

Combinatorial materials science (CMS) methods represent a powerful technique to produce a large number of compositions on a spatially addressable substrate. In particular, one may produce a continuous variation in composition across a substrate using physical vapor deposition techniques. For example, one can locate three evaporation targets at the vertices of a triangle to prepare a ternary phase diagram (Kennedy et al, 1965); or four targets at the corners of a square to prepare a quaternary phase diagram (van Dover et al, 1998) by sputter deposition. The drawback of this approach is that a non-linear variation in composition is produced as a function of position on the substrate. In order to obtain a linear relationship which would allow for a much easier interpretation of the data, we altered the flux produced by sputtering targets through design of masks which intercept the flux to create a linear or constant deposition as a function of position. Although CMS methods have been used to show that particular superconducting phases can be prepared (Xiang et al, 1995), to the author's knowledge the composition spread approach has not been used for this purpose until recently by our group (Sanderson and Hewitt, 2005, 2007) and subsequently by a Brookhaven group (Logvenov et al, 2007) using molecular beam epitaxy.
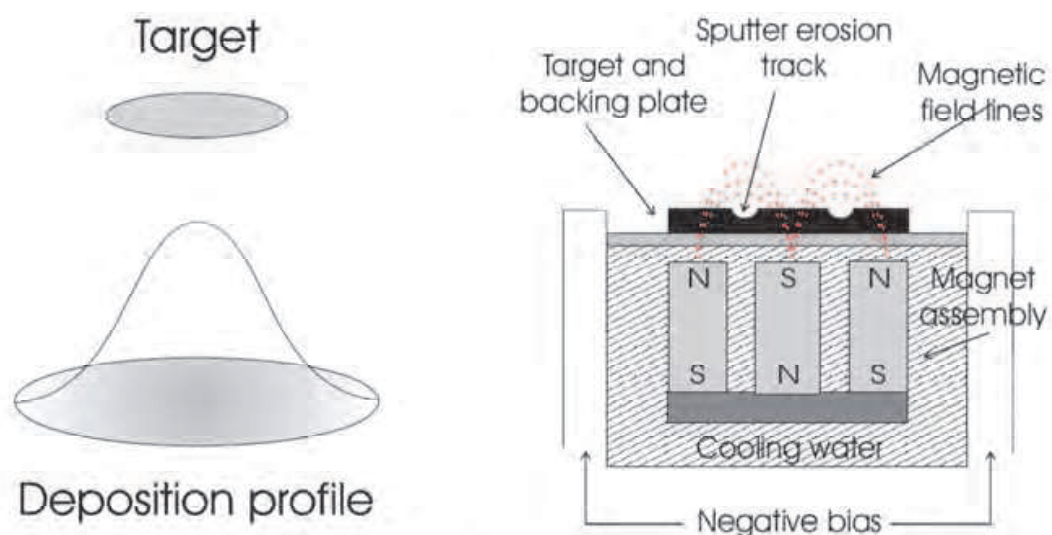

Fig. 1. Schematic showing the sputter flux generated by sputtering a circular target with a circular magnetron.

To implement a linear composition spread approach, the target deposition profile needs to be altered to provide the appropriate linear (or constant) variation across the substrate. One way to produce this variation is to interrupt the flux with a physical mask placed over the target. The process of determining the target mask profiles, for the Corona Vacuum Coaters V-3T sputtering system used in our lab is described in detail here, as outlined elsewhere (Dahn et al, 2002).

The sputtering flux from a circular magnetron can be determined by sputtering a target in front of a stationary substrate and measuring the mass as a function of position. The result for an aluminum target sputtered in an argon atmosphere at 5.6 mTorr is shown in Figure 2. A Gaussian profile of the form $J(q) = Ae^{-(q/w)^2}$ fits the data well, with the full width at half-max, $\omega = 10$ cm.
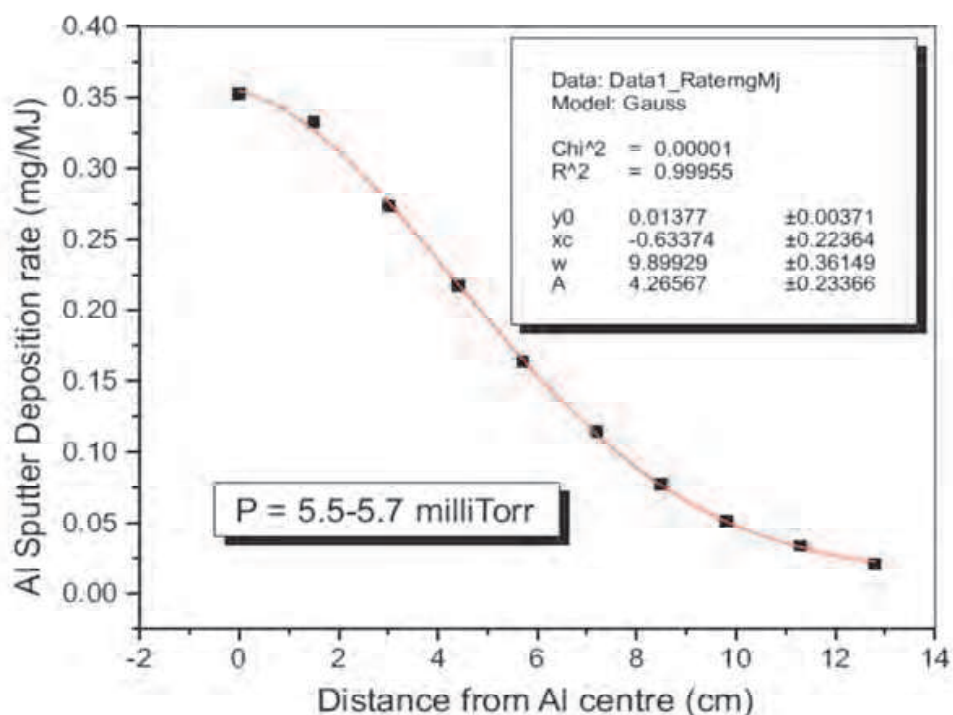

Fig. 2. Mass deposited per unit energy for an aluminum target sputtered in front of a stationary substrate table in a chamber with 5.6 mTorr Argon.

To intimately mix the elements the table must be rotated at a high rate, so one must calculate the deposition a rotating substrate. To obtain a specific deposition profile (linear out, linear in, constant) one must be able to calculate the amount of material deposited upon a rotating substrate, through a target mask. Figure 3 illustrates the geometry of the problem in which vectors $\mathbf{r_T}$ (table centre to target centre location on the table), $\mathbf{r_1}$ (from table centre to start of the deposited film) and $\mathbf{r_2}$ (distance from the table centre to the film end) are drawn. If $\mathbf{r_1}$ and $\mathbf{r_2}$ are equidistant from r_T, then the deposition would be the same at $\mathbf{r_1}$ and $\mathbf{r_2}$ when the substrate table is stationary. However, when the table is rotating, a point at $\mathbf{r_1}$ has a smaller tangential velocity than a point at $\mathbf{r_2}$, so more flux needs to reach $\mathbf{r_2}$ to produce the same deposition. For the Corona Vacuum Coaters V-3T sputtering system $\mathbf{r_T} = 13.33$ cm, $\mathbf{r_1} = 9.5$ cm and $\mathbf{r_2} = 17.1$ cm.

To calculate the mask profile needed consider the geometry shown in Fig. 3B. **R** is a vector from the centre of the substrate table to a point below the centre of the target on the table, while **q** is a vector from the centre of the target to the point on the substrate where the flux is being calculated. By integrating the flux along the heavy arc shown in Figure 3B the deposition D(s) can be found.
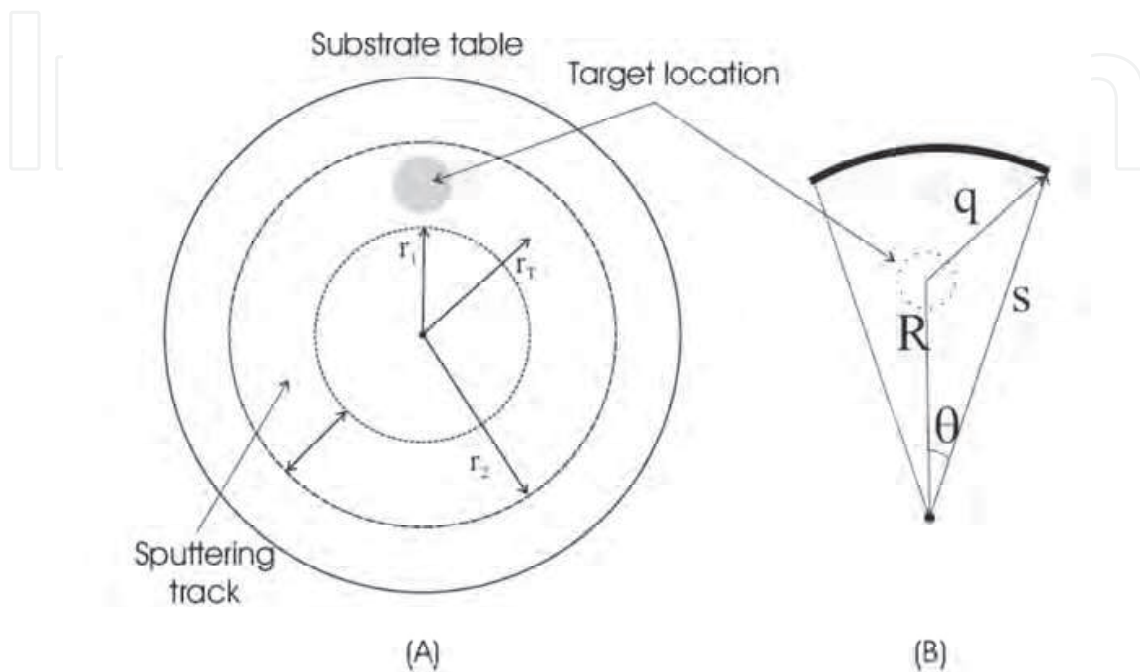

Fig. 3. Vectors defining important locations on the substrate table (A) and those needed to define the target mask (B).

It can be shown easily that,

$$q = \sqrt{R^2 + s^2 - 2sR\cos\theta} \tag{1}$$

and the deposition as a function of radial position (s) is,

$$D(s) = \int_0^{\theta_{max}} e^{-\left(\frac{q}{\omega}\right)^2} s\, d\theta \tag{2}$$

The expression of D(s) can be used to determine the desired deposition profile, whether linearly increasing or decreasing with s, or simply a constant independent of s. Finally, the mask shape can be numerically determined by solving Equations 1 and 2 for θ_{max} and s. The mask shape is found by converting the θ_{max} and s values to x and y coordinates. Masks have been designed for a constant deposition, as well as depositions that vary linearly, increasing inwards and outwards. With these three masks a wide variation of film compositions can be made. Figure 4 shows an image of each mask as well as masses of the film deposited onto a rotating substrate through the corresponding mask.

The results presented in the next section usually employ the set-up depicted in Figure 5. Using targets of composition A (placed behind the linear-in mask, blue in Fig. 5) and B (placed behind the linear out mask, red in Fig. 5), results in compositions varying linearly as $A_{1-x}B_x$ with radial position (s).
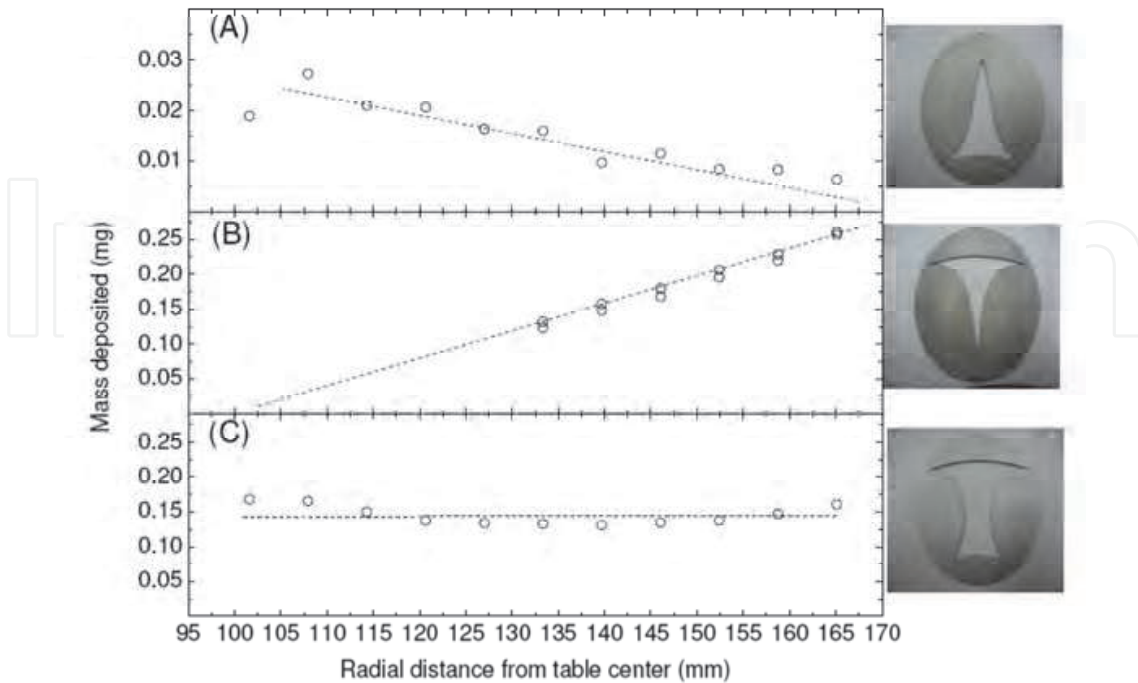
Fig. 4. Mass deposited through the linear in, linear out and constant masks. The dashed lines are a guide to the eye.
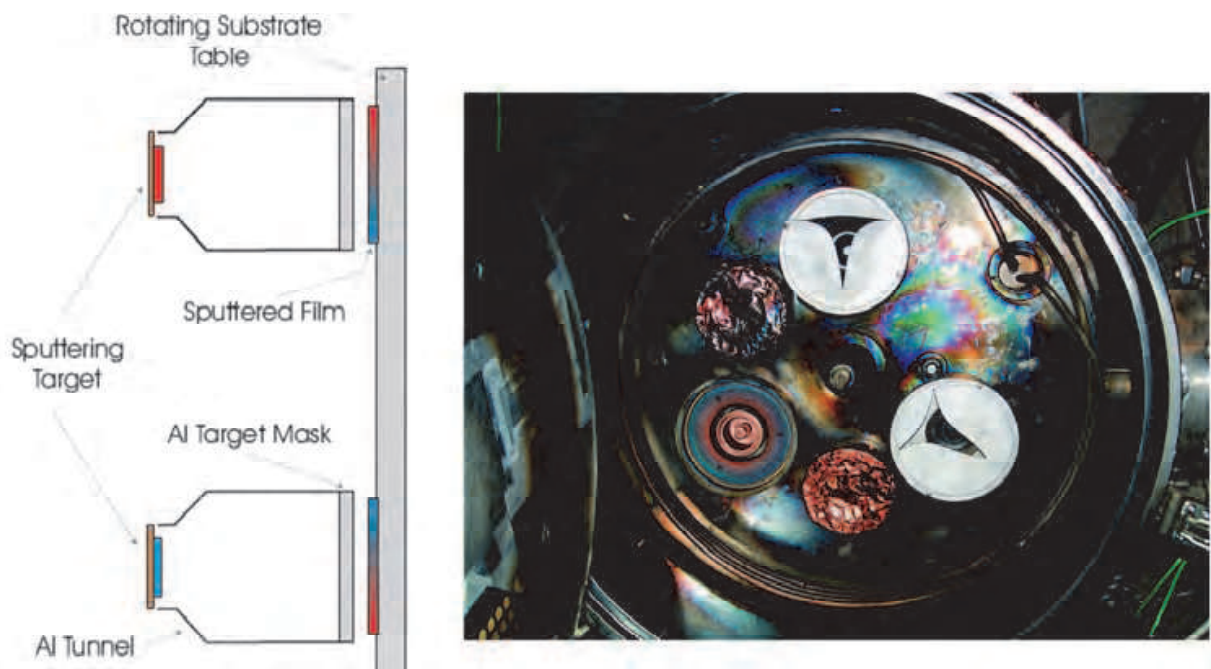

Fig. 5. Schematic side view (left) and actual (right) front-view image of the sputtering machine set-up with linear-in (at 4:00) and linear-out (at 12:00) masks placed in front of each target (color on-line).

3. Densely mapping the phase diagram of the cuprate superconductors

We first applied the linear composition spread approach to the cuprate superconductor Bi2212 (Sanderson and Hewitt, 2005, 2007), and then La214 (Saadat and Hewitt, 2010). The results for La214 are described here.

The cuprates are doped antiferromagnetic Mott-Hubbard insulators, becoming Fermi liquid metals at large hole concentrations. (They can also be electron doped, although the T_c's are not as high, reflecting some type of electron-hole asymmetry.) The limiting regimes are well described by the two-dimensional Hubbard model (Hubbard, 1963). When the onsite coulomb repulsion (U) dominates the kinetic energy of hopping (t) (U>>t), the solutions to the Hubbard Hamiltonian produce highly localized electron wavefunctions which gives rise to an insulator, and super-exchange interaction produces the Néel state. When the hopping term (t) dominates (t>>U), the solution is a modified Bloch wave function which gives rise to the Fermi liquid state. At intermediate hole concentrations where t and U are comparable, the transition from localized to itinerant electrons produces interesting physics and remains enigmatic. It is within this region of the phase diagram where superconductivity occurs. Thus it is important to understand the normal state properties of metal-insulator transitions (Mott, 1968), in order to decipher the nature of the superconducting state. Also, in this region of phase space there exists a partial suppression of low energy excitations, a Pseudogap (PG) (Timusk and Statt, 1999), which appears below a temperature $T^* > T_c$. Its exact description is a subject of intense study because it may hold the key to understanding the transition to the superconducting state. Theories of the PG can be divided into two broad categories: ones which identify it as a precursor to the onset of superconductivity, or others which classify it as a competing phase. It is thought that a dense map of the doping dependence of T^* is the key to deciphering the nature of the PG (Norman et al, 2005). Whether T^* merges with T_c in the overdoped regime or ends at optimal doping determines whether the PG is a "friend" or "foe" of superconductivity.

We have recently obtained data showing that one can densely map the temperature-hole concentration phase diagram of $La_{2-x}Sr_xCuO_{4+\delta}$ ($0 \leq x \leq 0.18$) using the spatial composition spread approach, as described in section 2 of this chapter, and presented in our recent article (Saadat et al, 2010). First applied to the cuprate superconductor Bi2212 (Sanderson and Hewitt, 2005, 2007), it was used to synthesize a $La_{2-x}Sr_xCuO_{4+\delta}$ ($0 \leq x \leq 0.18$) library. In this approach, targets of La_2CuO_4 and $La_{1.82}Sr_{0.18}CuO_4$ were co-sputtered with specially designed target masks, which ultimately produce a linear composition gradient varying from x = 0 (at 0 mm) to x = 0.18 (at 75 mm) on a set of eight single crystal substrates. The libraries' structures are characterized by X-ray diffraction (Fig. 6) and cation composition by Energy and Wavelength Dispersive Spectroscopy (EDS/WDS) (Fig. 7).

While we have shown it is possible to prepare single phase films in this manner, they are polycrystalline. Epitaxial films are required to separate contributions to T^* from c-axis and ab-plane transport. Polycrystalline films are sufficient, however, to measure T_c. Therefore, a high-throughput resistivity apparatus (Hewitt et al, 2005) was used to measure the DC resistivity of the 52 member library.

T_c and T^* were determined and plotted versus Sr content as shown in Fig. 9. We found that T_c is suppressed near 1/8 (x = 0.125) doping, consistent with the formation of a stripe phase (Tranquada et al, 1995). The lowest Sr content (x) at which superconductivity appears is 0.03, not at the expected value of 0.05 (Ando et al, 2004). Independent measurements of the hole
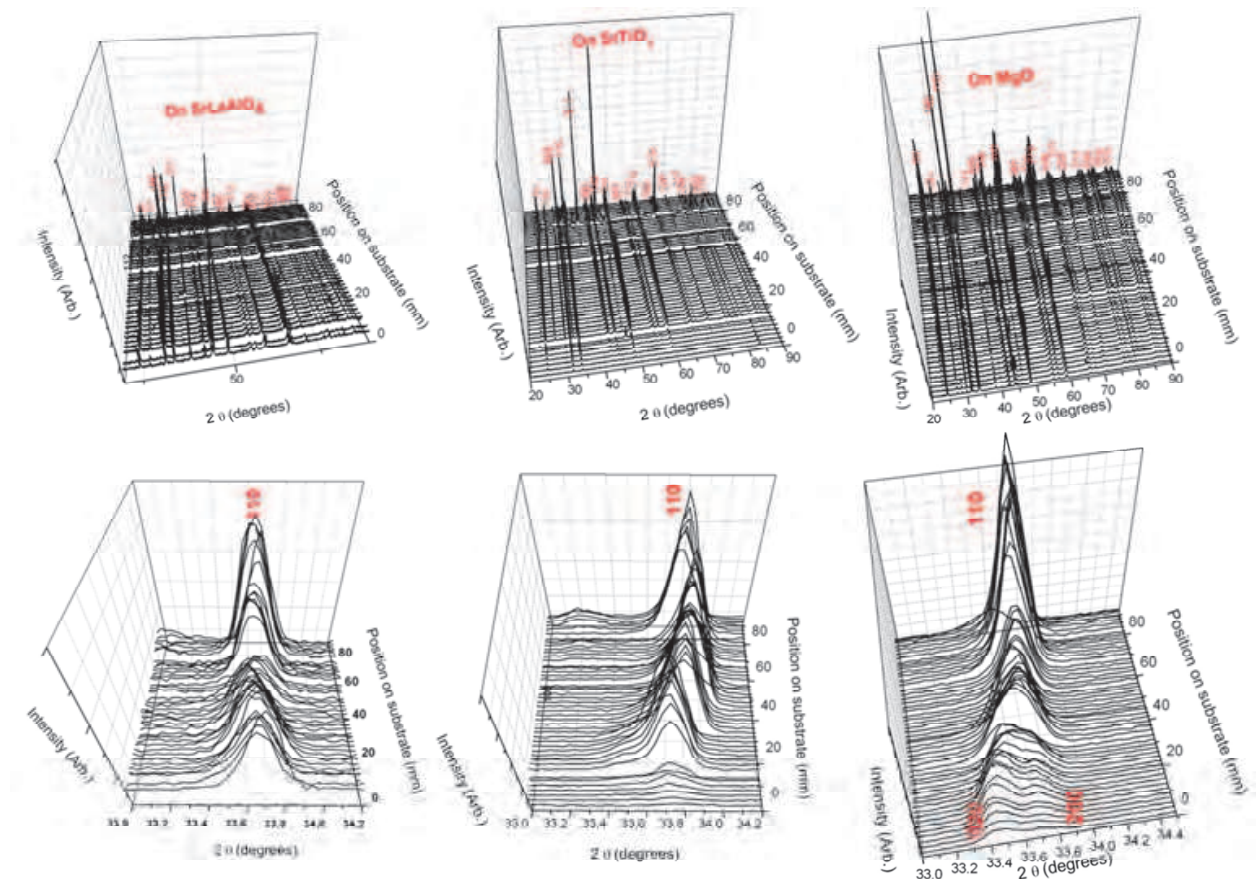
Fig. 6. X-ray diffraction of film library deposited onto three substrates (SrLaAlO$_4$, SrTiO$_3$ and MgO). The results (top panel of three) show the peaks can all be indexed to the La214 compound, and in the bottom panel of three the region where peaks sensitive to the tetragonal to orthorhombic phase transition ([110] – [020/200]) are found.
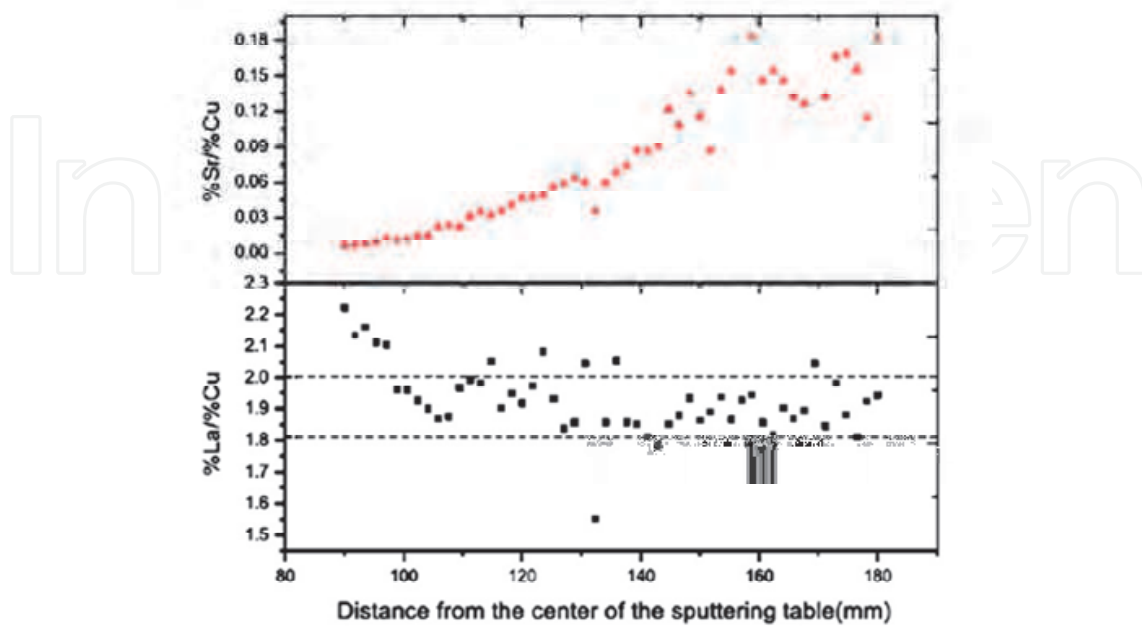

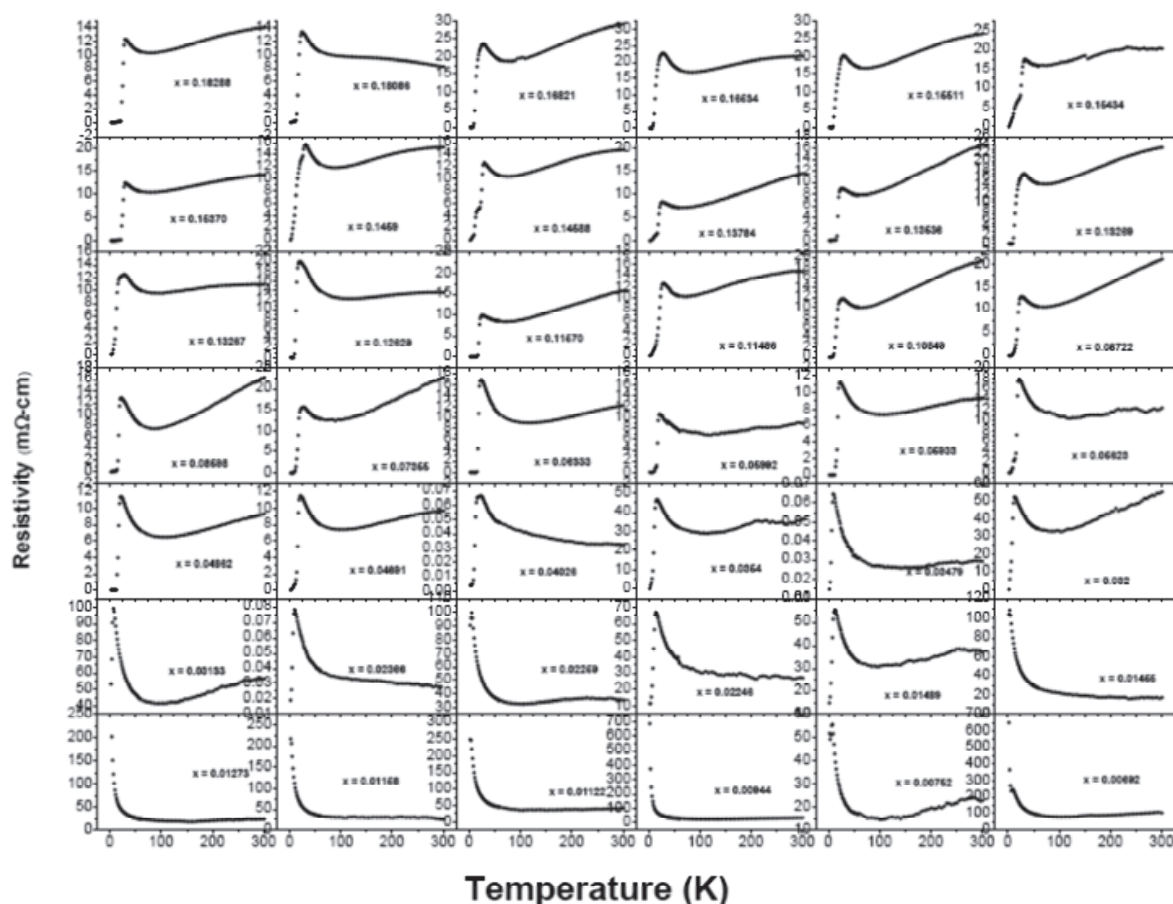Fig. 7. Elemental composition of the La$_{2-x}$Sr$_x$CuO$_4$ (0<x<0.18) library on MgO (100).

Fig. 8. The DC resistivity of the $La_{2-x}Sr_xCuO_4$ (0<x<0.18) library deposited onto $SrLaAlO_4$ substrates.

concentration can be obtained by measuring the intensity of a feature located 2 eV below the O Kedge (530 eV) by X-ray absorption spectroscopy (XAS) (Kuiper et al, 1988). These measurements would not only allow us to evaluate whether this unexpected result is a truly novel feature and not simply a consequence of oxygen non-stoichiometry and/or film strain, it would also test a theory that predicts the existence of charge 2e bosons in the PG state (Leigh et al, 2007; Choy et al, 2008).

4. Prospective 2D antiferromagnetic and ferromagnetic superconductors

In this chapter we also propose promising hosts for superconductivity and describe the use of the combinatorial approach to rapidly and efficiently scan the horribly large phase space of possible dopings. In the field of superconductivity there are very few "right" substitutions which produce superconductivity, and then only over a rather limited range of dopings.

Until recently, the cuprates and heavy fermion systems have presented a rather unique example of superconductivity in doped antiferromagnets. The phase diagram of the recently discovered FeAs-based (e.g. RE(O,F)FeAs, RE = La, Sm, or Ce (Luetkens et al, 2009; Drew et al, 2009; Zhao et al, 2008) and $(Ba,K)Fe_2As_2$ (Chen et al, 2009) superconductors share many features with the cuprates: a) they are doped antiferromagnets, b) superconductivity occurs
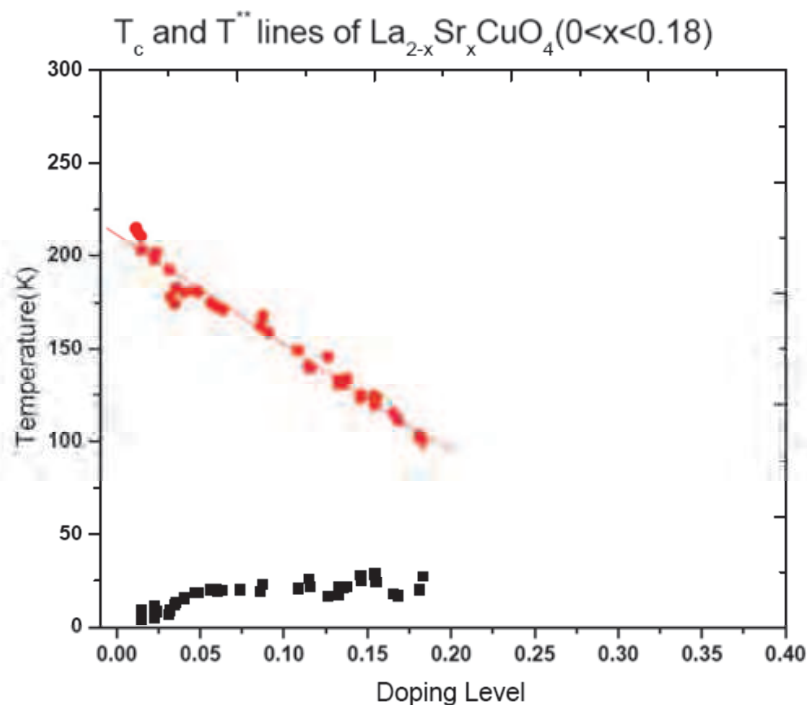
Fig. 9. T_c and T^* derived from the resistivity data of Fig. 8, for a La$_{2-x}$Sr$_x$CuO$_4$ (0<x<0.18) library deposited onto SrLaAlO$_4$ substrates using the spatial composition spread approach.

in 2D planes, though corrugated in FeAs-based materials, c) the planes are doped by adjacent charge reservoir layers, and d) the maximum superconducting transition temperature is a similar fraction (~1/3) of the maximum Néel temperature. Recent re-examination of the fulleride (A$_3$C$_{60}$; A = K, Cs, and Rb) superconductors has revealed that they are also doped antiferromagnetic insulators (Arvanitidis , 2007; Takabayashi, 2009). The phase diagram of cobaltate (Na$_x$CoO$_2$.yH$_2$O) (Foo et al, 2004; Takada et al, 2003) and heavy fermion (e.g. CeCoIn$_5$) (Petrovic et al, 2001) materials have this property as well.

A consistent picture is emerging (Uemura, 2009) that unconventional superconductivity is intimately related to antiferromagnetism (Fig. 10). Imai and coworkers have shown recently (Imai, 2009) that the strength of antiferromagnetic spin fluctuations in FeSe are correlated with the pressure-induced increase in T_c, suggesting a link between spin fluctuations and the mechanism of superconductivity, and have prompted some to suggest that it is a common thread linking organic, heavy-fermion, actinide, cuprate and Fe superconductors (Scalapino, 2009; Uemura, 2009). Spin fluctuation mediated pairing has always been a strong candidate for the mechanism of superconductivity in the cuprates, among the more than twenty candidates (Cho, 2006).

Monthoux and Lonzarich have proposed (Monthoux & Lonzarich, 1999; Monthoux & Lonzarich, 2001; Monthoux et al, 2007) a spin fluctuation based mechanism for superconductivity in systems close to a ferromagnetic or antiferromagnetic instability, making the convincing argument that on the border of long-range magnetic order the dominant interaction channel must be of magnetic origin and depend on the relative spin orientations of the interacting quasiparticles. Superconductivity is predicted to be more robust in doped antiferromagnets vs ferromagnets, and the amplitude of the oscillations in the interaction is enhanced by low dimensionality. For example, the range of temperature and pressure over which superconductivity is observed was increased by about one order of
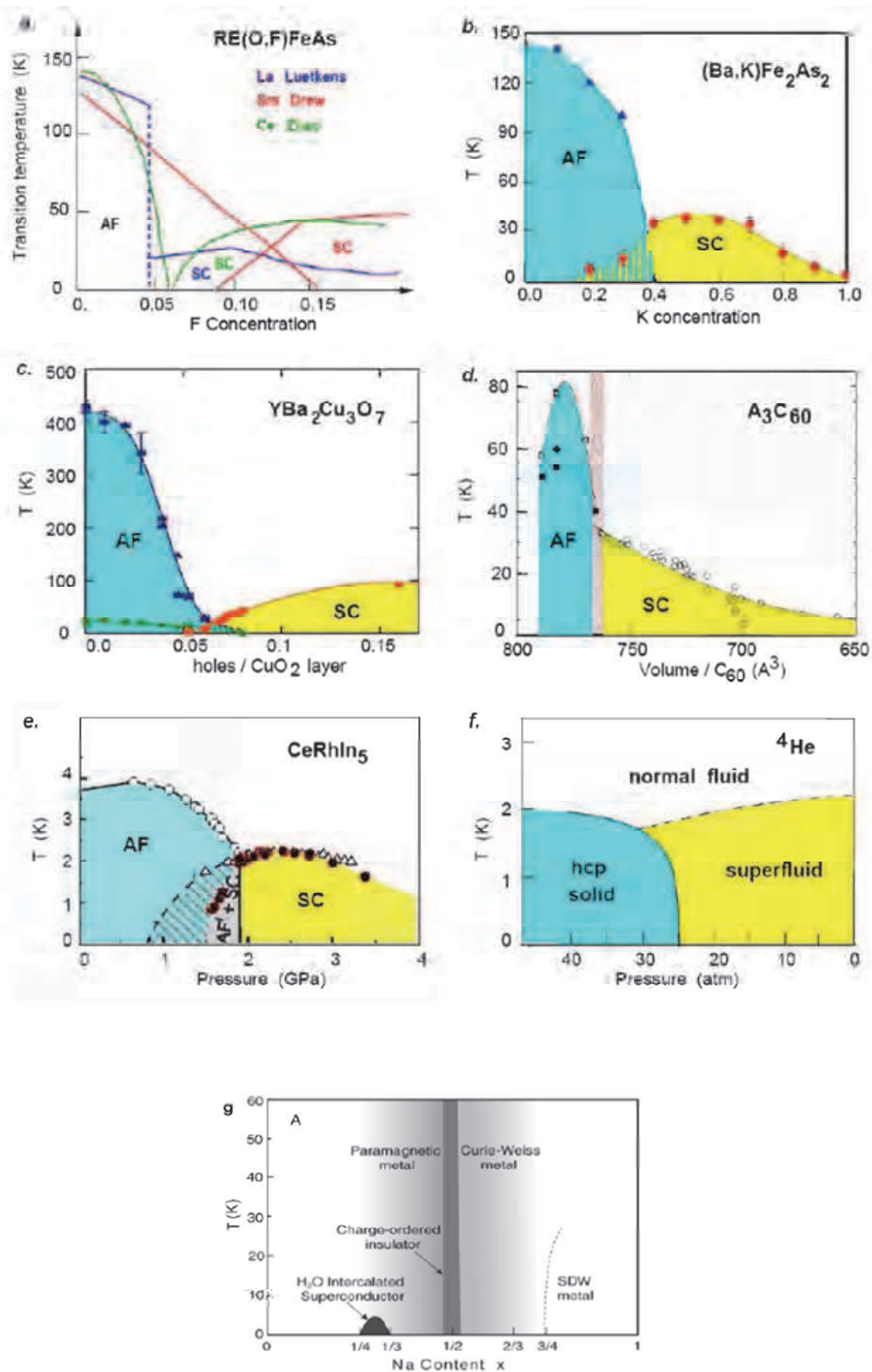
Fig. 10. Phase diagram of (a) RE(O,F)FeAs, (b) (Ba,K)Fe$_2$As$_2$, (c) YBa$_2$Cu$_3$O$_7$, (d) A$_3$C$_{60}$, (e) CeRhIn$_5$, (f) ^{4}He and (g) Na$_x$CoO$_2$.yH$_2$O demonstrating the proximity of superconducting and AF phases (adapted from Uemura, 2009).

magnitude in going from cubic $CeIn_3$ to its tetragonal analogues $CeMIn_5$ (M = Rh, Ir or Co) as anticipated by the magnetic interaction model (Monthoux & Lonzarich, 2002). Thus in the search for higher temperature superconductors one should explore the border of antiferromagnetism in a quasi two-dimensional tetragonal system with high characteristic spin fluctuation frequencies.

The conditions favourable for magnetic pairing include: (i) strong quasi two-dimensional antiferromagnetic correlations (large J) for spin singlet pairing and for large amplitude oscillations of the spin-spin interaction (gives small correlation length ξ which is inversely proportional to T_c), (ii) a single band of relatively high characteristic energy scale, and (iii) a crystal structure that enables the repulsive regions of the pairing potential to be optimally neutralized. Favourable T_c's can be achieved in layered d-electron systems of moderate electron densities (n) and bandwidths (t) and can be controlled by chemical doping or hydrostatic pressure (Monthoux et al, 2007).

One system which satisfies most of these requirements is the perovskite-type single layer compounds of composition A_2MX_4 and double layer compounds of composition $A_3M_2X_7$, where A^{1+} = K, Rb, Cs, M^{2+} = Mg, Mn, Fe, Co, Cu, Cd and X = F, Cl , or Br (see Geick, 2001 for a review). In these perovskite-type layer structures the dominant magnetic interaction is the nearest-neighbour Heisenberg exchange within the layers which causes their 2D character. These compounds have a metal ion (M) surrounded by 6 halides (X) in an octahedral arrangement. The magnetic properties depend on the intralayer superexchange interaction (J) mediated by the halide (X) between two M ions. Theory predicts an exponential dependence of J on the nearest neighbour distance (a_{MXM}) and experiments find a power law dependence $J(a_{nn}) = J(a_{nn,0})(a_{nn}/a_{nn,0})^{-12}$ for small a_{nn}.

A classic perovskite layer compound is La_2CuO_4 ($X = O^{2-}$, $M = Cu^{2+}$, and $A = La^{2+}$) which when appropriately doped (e.g. hole doped by replacing Sr^{2+} for La^{3+} or electron doped by replacing La^{3+} with Nd^{3+} and doping with $Ce^{3+,4+}$) forms a high temperature superconductor. It must be noted that *a priori* one could not have predicted these dopings would produce superconductivity. La_2CuO_4 has AFM order in-plane and out of plane and it is thought that superconductivity above liquid helium temperatures are possible because of (a) the large exchange interaction $J/k_B \sim 766$ K (Hayden et al, 1991); and (b) that the electrons in the Cu $d_{x^2-y^2}$ band possesses the correct symmetry to avoid Coulomb repulsion.

In looking for promising hosts, the single layer K_2CuF_4 and double layer $K_3Cu_2F_7$ compounds seem to have the right structure, and the d-band of Cu is the highest partially filled band. However, the intralayer interaction is small ($J/k_B = 11K$), produces ferromagnetic order (Feldkemper et al, 1995) and the Cu^{2+} ions exhibit alternating occupation of $z^2 - x^2$ and $z^2 - y^2$ hole states unlike the $x^2 - y^2$ ordering in La_2CuO_4 (Fig. 11). However, by inducing distortive changes at pressures larger than 9.5 GPa in the basal plane of the CuF_6 octahedra (Ishizuka et al, 1996; Ishizuka et al, 1998) was able to obtain (Fig. 12) antiferromagnetic order in K_2CuF_4 with $x^2 - y^2$ hole orbital overlap, exactly as found in the prototype cuprate superconductor La_2CuO_4.

SCAN PHASE SPACE: Since the high pressure phase of K_2CuF_4 is so similar to La_2CuO_4 in its orbital ordering, structure and magnetic properties, it satisfies the conditions set out by Monthoux and Lonzarich and should become a superconductor when appropriately doped. To obtain the high pressure phase of K_2CuF_4 one may attempt (a) pseudomorphic growth of
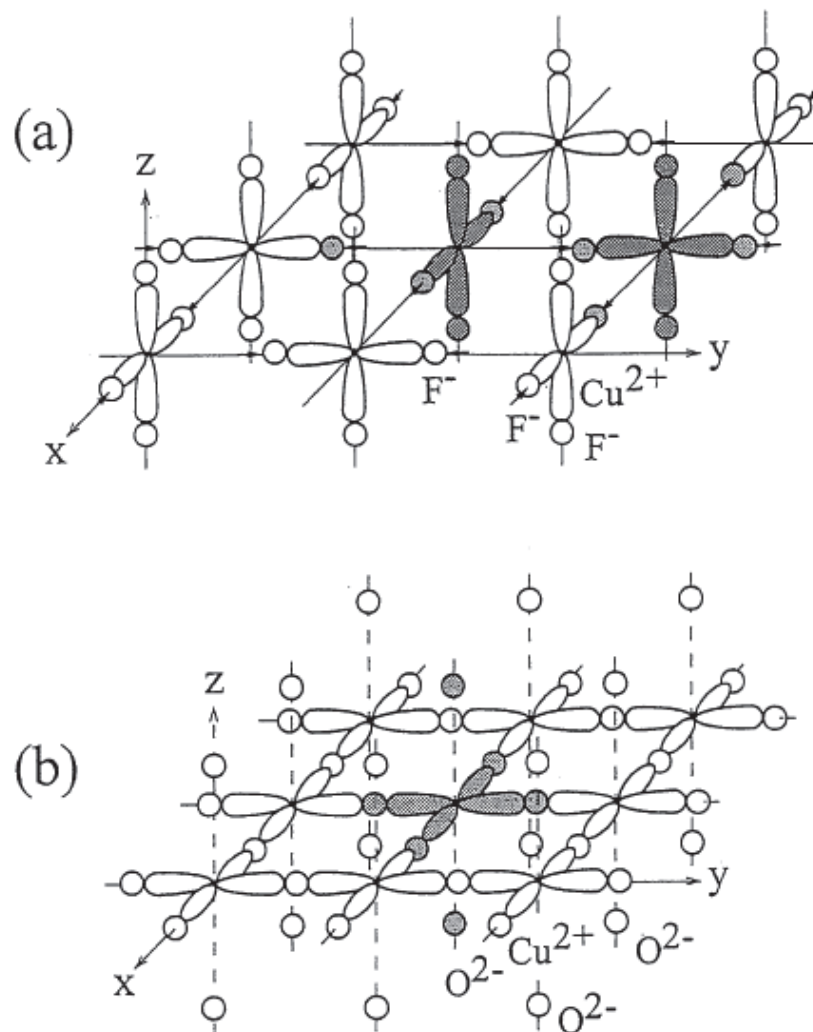
Fig. 11. The two kinds or orbital ordering in the basal plane of a K_2NiF_4-type compound. (a) Antiferrodistortive orbital ordering of $d_{x^2-z^2}$ and $d_{y^2-z^2}$ in K_2CuF_4 and (b) Ferrodistortive orbital ordering of $d_{x^2-y^2}$ in La_2CuO_4. In (a) the CuO_6 octahedra elongate alternately along a- and b-axis whereas it elongates along the c-axis only in (b). (from Ishizuka et al, 1996).

films onto substrates which produce compressive strain. The M-X-M distance in K_2CuF_4 is ~ 4.124 Å. Therefore, $SrLaAlO_4$ (3.756 Å, -10%), SrTiO3 (3.905 Å, -6%), $LaAlO_3$ (3.821 Å, -8%) and $SrLaGaO_4$ (3.843 Å, -8%) substrates should all produce compressive strain, while MgO (a = 4.212 Å, +1%) should produce tensile strain in epitaxial films. It must be noted that film stresses of more than 10 GPa have been achieved in pseudomorphic Fe layers (Sander, 1999). Epitaxial films of the cuprate superconductors sometimes show enhanced T_c perhaps because of the increase in J. One may also (b) dope smaller cations (Na^+, Li^+) to create pressure by cation substitution. Substrate or cation-induced decreases in the nearest neighbour M-X-M distances should also exponentially enhance the intra-layer interaction. In addition, we plan to replace the fluorine anion with other halides (Cl , Br , I) to enhance our understanding of the effect of the exchange interaction on the appearance of superconductivity in the films.
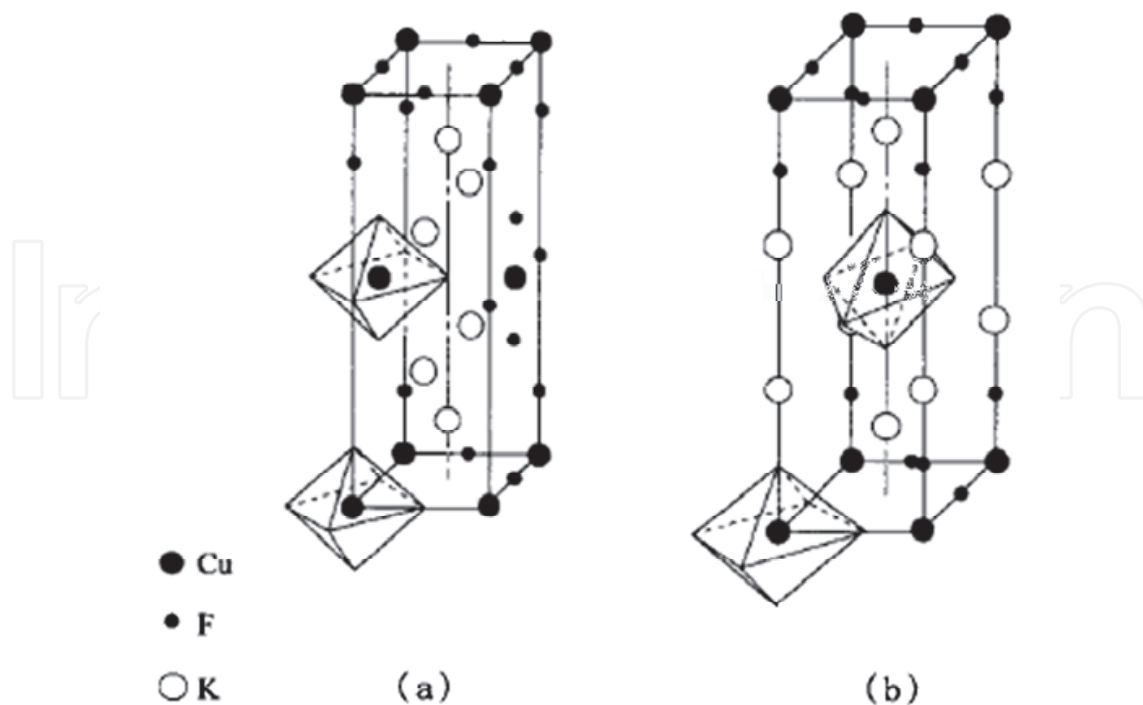
Fig. 12. The structures of K_2CuF_4 in (a) the high pressure phase (P>8GPa), and (b) at ambient pressure (from Ishizuka et al, 1998).

As pointed out earlier, it is difficult to predict *a priori* which doping would produce superconductivity, even when you've selected the right host. This is where the use of combinatorial methods to explore phase space rapidly and efficiently becomes a great asset. One should be able to replace K with higher valent cations C = Mg, Ca, Sr, Ba or Y, La to introduce carriers and produce the phases $K_{2-x}C_xCuF_4$ (0<x<2). Our 52-sample mask produces 52 unique compositions to be tested. In addition, K may be replaced with other alkali elements (A = Na, Li, Rb, Cs) at the same time to yield $(K_{1-y}A_y)_{2-x}C_xCuF_4$ phases (0<y<1, 0<x<2), which ultimately produces 52 x 52 = 2,704 unique compositions in one experiment. Every phase can then be tested for superconductivity using a high throughput resistivity apparatus. The full composition range of a pair of substituents (A, C) can be deposited in one sputtering run. Where superconductivity is found one can then explore phase space in the interesting region at higher density, followed by conventional solid state reaction techniques to produce the bulk phases. For every pair of elements A (5 choices) and C (6 choices) 2,704 unique compositions are created. With 30 different dopant pairs A-C we therefore produce 81,120 unique phases. If we have chosen the right host the probability of finding a superconductor should be nonzero. Assuming a very conservative 0.1% probability of finding superconductivity one should discover 81 superconducting phases. Each dopant pair requires at least 3 months to investigate fully, so 7.5 years are required to cover 30 pairs. Paul Canfield (Ames Lab and Iowa State U.) said (Canfield, 2008), "In deference to the term 'fishing trip', a real fisherman goes where the fish are known to congregate and reaps an abundant harvest." By casting our net wide, in the right host, it is **very likely** that the exploration described here will discover novel superconducting phases.

5. Conclusions

New materials form the basis of new products which drive economic development. Superconducting materials have held great promise for some time because they pass a current without resistance and expel magnetic fields. These properties make them the most sensitive magnetic sensors, best source of large magnetic fields (e.g. for use in medical imaging - MRI), most efficient transmisson lines; and are a leading candidate for high speed quantum computers (B. G. Levi, 2009). However, they have not found widespread application mainly because the materials require cooling to at least -136 degrees C. Finding materials that superconduct at much higher temperatures is now thought to be a realistic goal with the recent discovery of superconductivityin iron arsenide based materials, the observation that a number of superconductors are doped antiferromagnets, and the tremendous progress researchers have made in understanding the physical properties of existing superconductors. These developments have re-ignited the field by offering a path to novel superconductors - explore the transport properties of doped antiferromagnets.

To explore the properties of a large number of samples, a spatial composition spread approach has been developed at Dalhousie to more quickly and efficiently prepare new materials. In a single experiment hundreds of compositions can be studied, whereas a serial preparation approach would take several years. We have described in this chapter the feasibility of the approach to densely map the physical properties of an existing superconductor, $La_{2-x}Sr_xCuO_4$. To identify novel superconductors, we have proposed that layered fluoride perovskite compounds be screened using the high-throughput resistivity apparatus developed in our labs. To enhance our understanding of existing superconductors we have also shown that the phase diagram can be mapped at very high density to deduce the doping dependence of a feature, the pseudogap onset temperature, which helps determine the class of theories that apply to the cuprate superconductors.

6. Acknowledgements

7. References

Ando, Y., Komiya, S., Segawa, K., Ono, S., & Kurita, Y. (2004). Electronic phase diagram of high-T_c superconductors from mapping of the in-plane resistivity curvature. *Phys. Rev. Lett.*, Vol. 93, No. 26, (December 2004), pp. 267001-1-4, ISSN 0031-9007

Arvanitidis, J., Papagelis, K., Takabayashi, Y., Takenobu, T., Iwasa, Y., Rosseinsky, M. J., & Prassides, K. (2007). Magnetic ordering in the ammoniated alkali fullerides $(NH_3)K_{3-x}$ Rb_xC_{60} (x=2,3). *J. Phys.: Condens. Matter,* Vol. 19, No. 38, (September 2007), pp. 386235-1-13, ISSN 0953-8984

Canfield, P. C. (2008) Fishing the Fermi sea. *Nature Physics,* Vol. 4, No. 3, (March 2008), pp. 167-169, ISSN 1745-2473

Chen, H., Ren, Y., Qiu, Y., Bao, W., Liu, R. H., Wu, G., Wu, T., Xie, Y. L., Wang, X. F., Huang, Q. & Chen X. H. (2009). Coexistence of of the spin-density wave and superconductivity in $Ba_{1-x}K_xFe_2As_2$. *Europhys. Lett.*, Vol. 85, No. 17006, (January 2009), pp. 17006-p1-p5, ISSN 0295-5075

Cho, A. (2006). High-T_c: The mystery that defies solution. *Science*, Vol. 314, No. 5802, pp. 1072-1075, ISSN 0036-8075

Choy, T.-P., Leigh, R. G., & Phillips, P. (2008). Hidden charge-2e boson: Experimental consequences for doped Mott insulators. *Phys. Rev. B,* Vol. 77, No. 10, (March 2008), pp. 104524-1-9, ISSN 1098-0121

Dahn, J. R., Trussler, S., Hatchard, T. D., Bonakdarpour, A., Mueller-Neuhaus, J. R., Hewitt, K. C., & Fleischauer, M. (2002). Economical Sputtering system to produce large-size composition-spread libraries having linear and orthogonal stoichiometry variations. *Chem. Mater.*, Vol. 14, No. 8, (July 2002), pp. 3519-3523, ISSN 0897-4756

Drew, A. J., Niedermeyer, C., Baker, P. J., Pratt, F. L., Blundell, S. J., Lancaster, T., Liu, R. H., Wu, G., Chen, X. H., Watanabe, I., Malik, V. K., Dubroka, A., Rossie, M., Kim, K. W., Baines, C., & Bernhard, C. (2009). Coexistence of static magnetism and superconductivity in $SmFeAsO_{1-x}F_x$ as revealed by muon spin rotation. *Nature Materials,* Vol. 8, No. 4, (April 2009), pp. 310-314, ISSN 1476-1122

Feldkemper, S., Weber, W., Schulenburg, J., Richter, J. (1995). Ferromagnetic coupling in non-metallic Cu^{2+} compounds. *Phys. Rev. B*, Vol. 52, No. 1, (July 1995), pp. 313-323, ISSN 0163-1829

Foo, M. L., Wang, Y. Y., Watauchi, S., Zandbergen, H. W., He, T., Cava, R. J., Ong, N. P. (2004). Charge ordering, commensurability, and metallicity in the phase diagram of the layered Na_xCoO_2. *Phys. Rev. Lett.*, Vol. 92, No. 24, (June 2004), pp. 247001-1-4, ISSN 0031-9007

Geick, R. (2001). Halide Perovskite-type Layer Structures (Subvolume J3), In*:. Group III: Condensed Matter – Volume 27, Magnetic Properties of Non-Metallic Inorganic compounds based on transition elements (Landolt-Börnstein: Numerical Data and Functional Relationships in Science and Technology),* H. P. J. Wijn, pp. 159-161, 188-190, 254, Springer-Verlag, ISBN 1616-9549, Berlin, Germany

Hayden, S. M., Aeppli, G., Osborn, R., Taylor, A. D., Perring, T. G., Cheong, S. W., Fisk, Z. (1991). High energy spin waves in La_2CuO_4. *Phys. Rev. Lett.*, Vol. 67, No. 25, (December 1991), pp. 3622-3625, ISSN 0031-9007

Hewitt, K. C., Casey, P. A., Sanderson, R. J., White, M. A. & Sun, R (2005). High-throughput resistivity apparatus for thin-film combinatorial libraries. *Rev. Sci. Instrum.,* Vol. 76, No. 9, (September 2005), pp. 093906-1-9, ISSN 0034-6748

Hubbard, J. (1963). Electron correlations in narrow energy bands. *Proc. Roy. Soc. Lon. A,* Vol. 276, No. 1365, (November 1963), pp. 257, ISSN

Imai, T., Ahilan, K., Ning, F. L., McQueen, T. M., Cava, R. J. (2009). Why does undoped FeSe become a high-T_c superconductor under pressure? *Phys. Rev. Lett.,* Vol. 102, No. 17, (May 2009), pp. 177005-1-4, ISSN 0031-9007

Ishizuka, M., Yamada, I., Amaya, K., & Endo, S. (1996). Change of magnetism in the two-dimensional Heisenberg ferromagnet K_2CuF_4 observed at high pressure. *J. Phys. Soc. Jpn.*, Vol. 65, No. 7, (July 1996), pp. 1927-1929, ISSN 0031-9015

Ishizuka, M. Terai, M., Endo, S., Hidaka, M., Yamada, I., & Shimomura, O. (1998). Pressure induced phase transition in the two-dimensional Heisenberg ferromagnet K_2CuF_4. J. *Magn. Mag. Mater.*, Vol. 177, No. 1, (January 1998), pp. 725-726, ISSN 0304-8853

Kennedy, K., Stefansky, T. Davy, G., Zakay, V. F. & Parker, E. R. (1965). Rapid Method for determining ternary-alloy phase diagrams. *J. Appl. Phys.*, Vol. 36, No. 12, (December 1965), pp. 3808-3810, ISSN 0021-8979

Kuiper, P., Kruizinga, G., Ghijsen, J., Grioni, M., Weijs, P. J. W., de Groot, F. M. F., Sawatzky, G. A., Verweij, H., Feiner, L. F., & Petersen, H. (1988). X-ray absorption study of the O 2p hole concentration dependence on O stoichiometry in $YBa_2Cu_3O_x$. *Phys. Rev. B*, Vol. 38, No. 10, (October 1988), pp. 6483-6489, ISSN 0163-1829

Leigh, R. G., Phillips, P., & Choy, T. P. (2007). Hidden charge 2e boson in doped Mott insulators. *Phys. Rev. Lett.*, Vol. 99, No. 4, (July 2007), pp. 046404-1-4, ISSN 0031-9007

Levi, B. G. (2009). Superconducting qubit systems come of age. *Physics Today*, Vol. 62, No. 7, (July 2009), pp. 14-16, ISSN 0031-9228

Logvenov, G., Sveklo, I., & Bozovic, I. (2007). Combinatorial molecular beam epitaxy of $La_{2-x}Sr_xCuO_{4+\delta}$. *Physica C,* Vol. 460, (September 2007), pp. 416-419, ISSN 0921-4534

Luetkens, H., Klaus, H. H., Kraken, M., Litterst, F. J., Dellmann, T., Klingeler, R., Hess, C., Khasanov, R., Amato, A., Baines, C., Kosmala, M., Schumann, O. J., Braden, M., Hamann-Borrero, J., Leps, N., Kondrat, A., Behr, G., Werner, J., & Buchner, B. (2009). The electronic phase diagram of the $LaO_{1-x}F_xFeAs$ superconductor. *Nature Materials,* Vol. 8, No. 4, (April 2009), pp. 305-309, ISSN 1476-1122

Monthoux, P. & Lonzarich, G. G. (1999) p-wave and d-wave superconductivity in quasi-two-dimensional metals. *Phys. Rev. B,* Vol. 59, No. 22, (June 1999), pp. 14598-14605, ISSN 0163-1829

Monthoux, P., & Lonzarich, G. G. (2001). Magnetically mediated superconductivity in quasi-two and three dimensions. *Phys. Rev. B,* Vol. 63, No. 5, (February 2001), pp. 054529-1-10, ISSN 0163-1829

Monthoux, P, Pines, D., Lonzarich, G. G. (2007). Superconductivity without phonons. *Nature,* Vol. 450, No. 7173, (December 2007), pp. 1177-1183, ISSN 0028-0836

Monthoux, P, & Lonzarich, G. G. (2002). Magnetically mediated superconductivity: Crossover from cubic to tetragonal lattice. *Phys. Rev. B*, Vol. 66, No. 22, (December 2002), pp. 224504-1-8, ISSN 1098-0121

Mott, N. (1968) Metal-Insulator Transitions. *Rev. Mod. Phys.*, Vol. 40, No. 4, (October 1968), pp. 677-683

Norman, M. R., Pines, D., & Kallin, C. (2005). The Pseudogap: friend or foe of high T_c? *Advances in Physics,* Vol. 54, No. 8, (December 2005), pp. 715-733, ISSN 0001-8732

Petrovic, C., Pagliuso, P. G., Hundley, M. F., Movshovich, R., Sarrao, J. L., Thompson, J. D., Fisk, Z., & Monthoux, P. (2001). Heavy-fermion superconductivity in $CeCoIn_5$ at 2.3

K. *J. Phys.:Condens. Mat.,* Vol. 13, No. 17, (April 2001), pp. L337-L342, ISSN 0953-8984

Saadat, M., George, A. E., & Hewitt, K. C. (2010). Densely mapping the phase diagram of cuprate superconductors using a spatial composition spread approach. *Physica C,* Vol. 470, No. Sp. Iss. SI Suppl. 1, (December 2010), pp. S59-S61, ISSN 0921-4534

Sander, D. (1999). The correlation between mechanical stress and magnetic anisotropy in ultrathin films. *Rep. Prog. Phys.,* Vol. 62, No. 5, (May 1999), pp. 809-858, ISSN 0034-4885

Sanderson, R. J. & Hewitt, K. C. (2007). Magnetron sputter deposition of a 48-member cuprate superconductor library: $Bi_2Sr_2Y_xCa_{1-x}Cu_2O_{8+\delta}$ ($0.5 \leq x \leq 1$) linearly varying in steps of $\Delta x = 0.01$. *Appl. Surf. Sci.,* Vol. 254, No. 3, (November 2007), pp. 760-764, ISSN 0169-4332

Sanderson, R. J. & Hewitt, K. C. (2005) Stoichiometry control of magnetron sputtered $Bi_2Sr_2Ca_{1-x}Y_xCu_2O_y$ ($0 \leq x \leq 0.5$), thin film, composition spread libraries: Substrate bias and gas density factors. *Physica C,* Vol. 425, No. 1-2, (September 2005), pp. 52-61, ISSN 0921-4534

Scalapino, D. J. 9th International Conference on Materials and Mechanism of Superconductivity. Tokyo, Japan, Sept. 10 (2009)

Takabayashi, Y., Ganin, A. Y., Jeglic, P., Arcon, D., Takano, T., Iwasa, Y., Ohishi, Y., Takata, M., Takeshite, N., Prassides, K., & Rosseinsky, M. J. (2009). The Disorder-free non-BCS superconductor Cs_3C_{60} emerges from an antiferromagnetic insulator parent state. *Science,* Vol. 323, No. 5921, (March 2009), pp. 1585-1590, ISSN 0036-8075

Takada, K., Sakurai, H., Takayama-Muromachi, E., Izumi, F., Dilanian, R. A., & Sasaki, T. (2003). Superconductivity in two-dimensional CoO_2 layers. *Nature,* Vol. 422, No. 6927, (March 2003), pp. 53-55, ISSN 0028-0836

Timusk, T. & Statt, B. (1999). The Pseudogap in high-temperature superconductors: An experimental survey. *Rep. Prog. Phys.,* Vol. 62, No. 1, (January 1999), pp. 61-122, ISSN 0034-4885

Tranquada, J. M., Sternlieb, B. J., Axe, J. D., Nakamura, Y., & Uchida, S. (1995). Evidence for stripe correlations of spins and holes in copper-oxide superconductors. *Nature,* Vol. 375, No. 6532, (June 1995), pp. 561-563, ISSN 0028-0836

Uemura, Y. J. (2009). Commonalities in phase and mode. *Nature Materials,* Vol. 8, No. 4, (April 2009), pp. 253-255, ISSN 1476-1122

Van Dover, R. B., Schneemeyer, L. F., & Fleming, R. M. (1998). Discovery of a useful thin-film dielectric using a composition-spread approach. *Nature,* Vol. 392, No. 6672, (March 1998), pp. 162-164, ISSN 0028-0836

Xiang, X. D., Sun, X.-D., Briceno, G., Lou, Y. L., Wang, K. A., Chang, H. Y., Wallacefreedman, W. G., Chen, S. W., & Schultz, P. G. (1995). A Combinatorial approach to materials discovery. *Science,* Vol. 268, No. 5218, (June 1995), pp. 1738-1740, ISSN 0036-8075

Xiang, X-D. (1999). Combinatorial materials synthesis and screening: An integrated materials chip approach to discovery and optimization of functional materials. *Annu. Rev. Mater. Sci.,* Vol. 29, pp. 149-171, ISSN 0084-6600

Zhao, J., Huang, Q., de la Cruz, C., Li, S. L., Lynn, J. W., Chen, Y., Green, M. A., Chen, G. F., Li, G., Li, Z., Luo, J. L., Wang, N. L., & Dai, P. C. (2008). Structural and Magnetic phase diagram of $CeFeAsO_{1-x}F_x$ and its relation to high-temperature superconductivity. *Nature Materials,* Vol. 7, No. 12, (December 2008), pp. 953-959, ISSN 1476-1122.
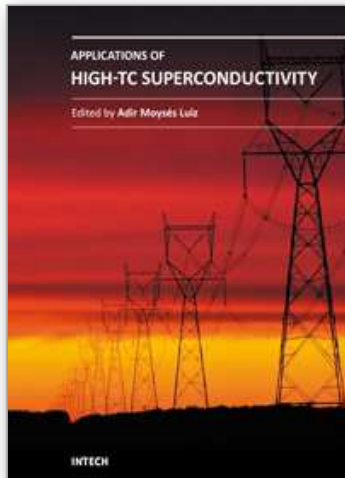
Applications of High-Tc Superconductivity
Edited by Dr. Adir Luiz

This book is a collection of the chapters intended to study only practical applications of HTS materials. You will find here a great number of research on actual applications of HTS as well as possible future applications of HTS. Depending on the strength of the applied magnetic field, applications of HTS may be divided in two groups: large scale applications (large magnetic fields) and small scale applications (small magnetic fields). 12 chapters in the book are fascinating studies about large scale applications as well as small scale applications of HTS. Some chapters are presenting interesting research on the synthesis of special materials that may be useful in practical applications of HTS. There are also research about properties of high-Tc superconductors and experimental research about HTS materials with potential applications. The future of practical applications of HTS materials is very exciting. I hope that this book will be useful in the research of new radical solutions for practical applications of HTS materials and that it will encourage further experimental research of HTS materials with potential technological applications.

How to reference

In order to correctly reference this scholarly work, feel free to copy and paste the following:

Kevin C. Hewitt, Robert J. Sanderson and Mehran Saadat (2011). Preparation of Existing and Novel Superconductors using a Spatial Composition Spread Approach, Applications of High-Tc Superconductivity, Dr. Adir Luiz (Ed.), ISBN: 978-953-307-308-8, InTech, Available from:
http://www.intechopen.com/books/applications-of-high-tc-superconductivity/preparation-of-existing-and-novel-superconductors-using-a-spatial-composition-spread-approach

INTECH
open science | open minds